Supplementary Information (SI) for Nanoscale Horizons.

Supporting Information

Tannic Acid-Mediated Surface Engineering of CNTs for Enhanced Bifunctional Oxygen Electrocatalysis

Xiangmin Tang, [a,b] Luyao Zou, [a] Xiaopeng Li [a,b], Zhipeng Xu,[c] Huilin Fan, [a,*] Chao Lin, [a,b,*] Jung-Ho Lee[c,*]

[a] School of New Energy, Ningbo University of Technology, Ningbo, 315336, China.

[b] State Key Laboratory of Advanced Fiber Materials, College of Materials Science and Engineering, Donghua University, Shanghai, 201620, P. R. China.

[c] Department of Materials and Chemical Engineering, Hanyang University, Ansan, Gyeonggi-do, 15588, Korea.

Experiment Section

Characterizations

Scanning electron microscopy (SEM) images were obtained using field emission scanning electron microscope (Hitachi SU8010, Japan). Transmission electron microscopy (TEM) and HAADF-STEM images were acquired using Talos F200S operated at 200 kV. AC HAADF-STEM characterization was performed on JEOL ARM200F and Themis ETEM installed with a CEOS probe corrector. The phase purity and crystallographic information of the materials were characterized by X-ray powder diffractometer (XRD, Bruker D2 Phaser diffractometer) using Cu Kα radiation (λ = 1.5406 Å). Brunauer-Emmett-Teller (BET) surface area of all samples were measured by N_2 adsorption and desorption at 77 K using an ASAP 2460 system. The samples were degassed offline at 200 °C for 12 h under vacuum before the analysis. And the pore size distribution was analyzed by NLDFT Advanced PSD. The Co content in the catalyst was conducted on the Inductively Coupled Plasma Mass Spectrometry (ICP-MS, iCAP-Q). Raman spectra were recorded on an InVia-Reflex spectrometer (Renishaw). The surface chemical compositions of the samples were analyzed using X-ray photoelectron spectroscopy (XPS, Escalab 250Xi). All XPS spectra were calibrated according to the C 1s line at 284.8 eV.

Electrochemical measurements

ORR measurement

The electrochemical tests were measured with a three-electrode system on an electrochemical workstation (Princeton Multichannel). A rotating disk glass carbon electrode (GCE, disk diameter of 5 mm with surface area of 0.196 cm^2) was used as the substrate for the working electrode, and a Pt wire and Ag/AgCl (3.5 M KCl) electrode were utilized as the counter electrode and the reference electrode, respectively. The rotating speed of RDE was 1600 rpm. The catalyst (5 mg) was dispersed in a mixed solution of ethanol (475 μL) and Nafion solution (25 μL), and then subjected to sonication for 1 hour to achieve a homogeneous distribution of the electrocatalysts. The catalyst ink (10 μL) was dropped on the RDE electrode and then dried in the air. All of the potentials were calibrated to the reversible hydrogen electrode (RHE) according to the Nernst equation

$$E_{RHE}= E_{Ag/AgCl} +0.2046+0.059\times pH$$

The electrolyte (0.1M KOH) was pre-purged with pure oxygen for at least 10 min to reach oxygen saturation and oxygen flow was kept during the electrochemical test.

Cyclic voltammetry (CV) measurements were conducted at a scan rate of 10 mV s^{-1}. The linear sweep voltammetry (LSV) measurements were conducted at a scan rate of 10 mV s^{-1}. Electrochemical impedance spectroscopy (EIS) measurements were evaluated with the frequency range from 100 kHz to 0.01 Hz. The ion diffusion coefficients were calculated according to

$$D_{\mathrm{OH}^-} = 0.5\left(\frac{RT}{n^2F^2AC\sigma}\right)^2$$

where R is the gas constant (8.314 J K^{-1} mol^{-1}), T is the room temperature (298.15 K), A is the surface area of the electrode (0.196 cm^{-2}), n is the number of electrons transferred (4), F is the Faraday constant (96485.33 C mol^{-1}), C is the concentration of OH^- (1×10^{-3} mol cm^{-3}), and σ is the slope of the plot of Z', against $\omega^{-1/2}$ based on $Z' = R_s + R_{ct} + \sigma\omega^{-1/2}$. When a rotating ring disk electrode (RRDE) was measured at 1.3 V (vs. RHE) with the rotating speed at 1600 rpm, electron transfer number (n) and hydrogen peroxide yield (% H_2O_2) were calculated through the following equations.

$$n = 4I_D / (I_D + I_R/N)$$

$$H_2O_2\% = 200 \times (I_R/N) / (I_D + (I_R/N)$$

where I_D and I_R are the disk and ring faradaic current, respectively, and N is the collection factor (0.37) of the ring electrode.

The kinetic current density (J_K) was calculated according to the Koutecky-Levich (K-L) equation:

$$\frac{1}{j} = \frac{1}{j_L} + \frac{1}{j_K} = \frac{1}{B\omega^{1/2}} + \frac{1}{j_K}$$

$$B = 0.62nFC_0(D_0)^{2/3}\nu^{-1/6}$$

Where, J, J_K and J_L represent the measured current density, kinetic current density, and diffusion limited current density, respectively, ω is the rotation speed of electrode, n is the ORR electron transfer number, F is the Faraday constant (96485 C mol^{-1}), C_0

is the oxygen-saturated concentration (1.2×10^{-3} mol L^{-1}), D_0 is the diffusion coefficient of O_2 (1.9×10^{-5} cm^2 s^{-1}), v is the kinetic viscosity of the electrolyte (0.01 cm^2 s^{-1}).

OER measurement

The electrochemical tests were measured with a three-electrode system on an electrochemical workstation (CHI1140D). A carbon paper was used as the substrate for the working electrode, and a Hg/HgO electrode were utilized as the counter electrode and the reference electrode, respectively. The catalyst (5 mg) was dispersed in a mixed solution of ethanol (480 μL) and Nafion solution (20 μL), and then subjected to sonication for 1 hour to achieve a homogeneous distribution of the electrocatalysts. The catalyst ink (50 μL) was dropped on the carbon paper (the effective surface area is 0.5 cm^{-2}) and then dried in the air. The potentials were calibrated to the reversible hydrogen electrode (RHE) according to the Nernst equation

$$E_{RHE}= E_{Hg/HgO} +0.098+0.059*pH$$

The linear sweep voltammetry (LSV) measurements were conducted at a scan rate of 10 mV s^{-1} in 1 M KOH electrolyte.

Zinc air batteries (ZAB) test

Liquid-state ZAB measurement

Liquid ZAB measurements were carried out using a homemade cell in a two-electrode configuration. The anode was made up of a polished Zn foil, while the air cathodes was prepared by coating Co-N/CNTs catalyst ink onto carbon paper, and the back was coated with a gas-diffusion layer, the catalyst loading was controlled to 1.0 mg cm^{-2}. The 6 M KOH solution containing 0.2 M zinc acetate was used as the electrolyte. Prior to performance tests, the electrolyte was also purged with oxygen for

30 min in order to saturate electrolyte with oxygen. The open circuit voltage, discharging and charging polarization curves were recorded using the CHI760E electrochemical workstation. Rate performance of the assembled ZAB were evaluated by recording voltage profiles during galvanostatic discharge at various current densities from 5 to 100 mA cm^{-2}. The constant current discharge-charge cycle curves of the batteries were carried out at room temperature using a battery test system (Land 3001A). The ZAB were discharged for 10 min and charged for 10 min at a current density of 5 mA cm^{-2} in each galvanostatic cycle.

All-solid-state ZAB measurement

Flexible solid-state ZAB is consisted of air electrode, solid electrolytes and zinc foil, respectively. The air electrode was a carbon paper layer coated with catalyst (catalyst loading of 1.0 mg cm^{-2}) on the electrolyte-facing side. The solid electrolytes adopted copolymers of acrylic acid (AA) and methacryloyloxyethyl trimethyl ammonium chloride (DMC). The polarization curves were recorded via linear sweep voltammetry (LSV) at room temperature on a CHI 760E electrochemical working station. The ZAB were discharged for 10 min and charged for 10 min at a current density of 2 mA cm^{-2} in each galvanostatic cycle.

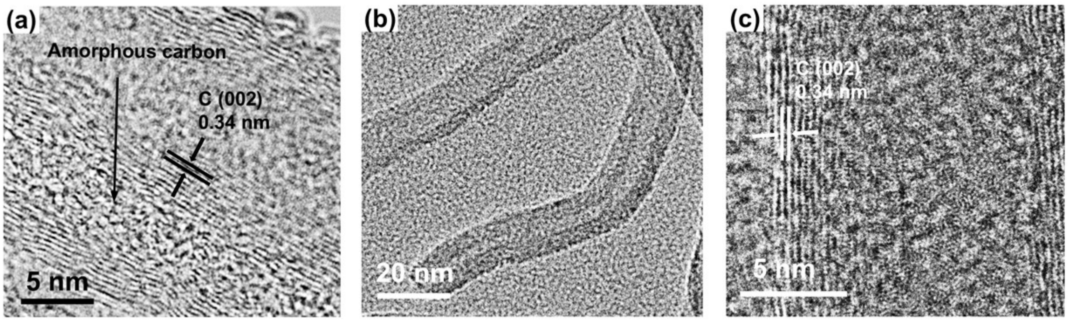

Fig. S1. (a) HR-TEM image of Co-N/CNTs-0.06, (b) TEM and (c) HR-TEM images of CNTs.

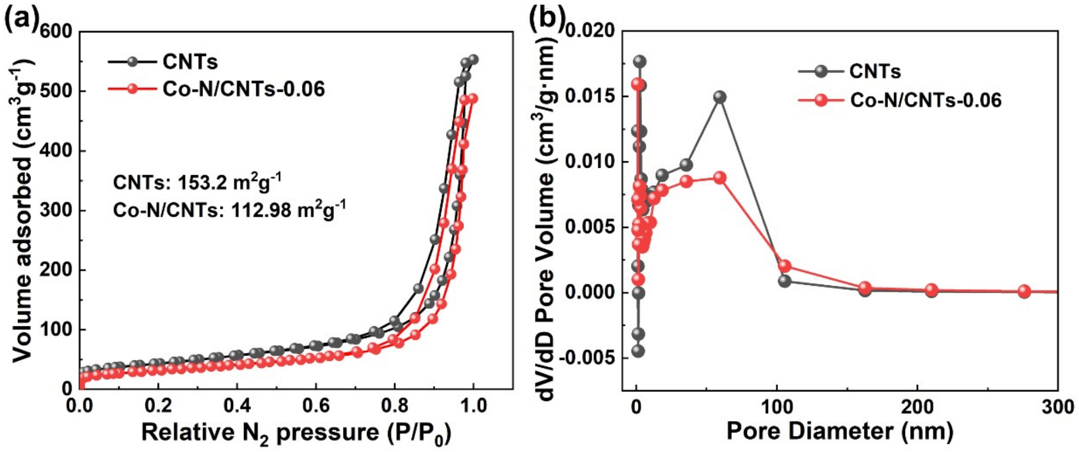

Fig. S2. The (a) N_2 adsorption-desorption isotherms and (b) pore size distribution of CNTs and Co-N/CNTs-0.06

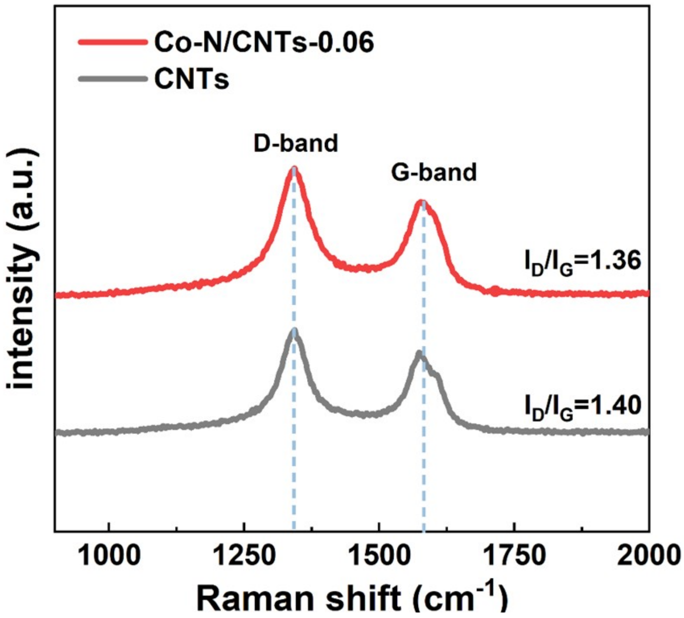

Fig. S3 Raman spectra of CNTs and Co-N/CNTs-0.06

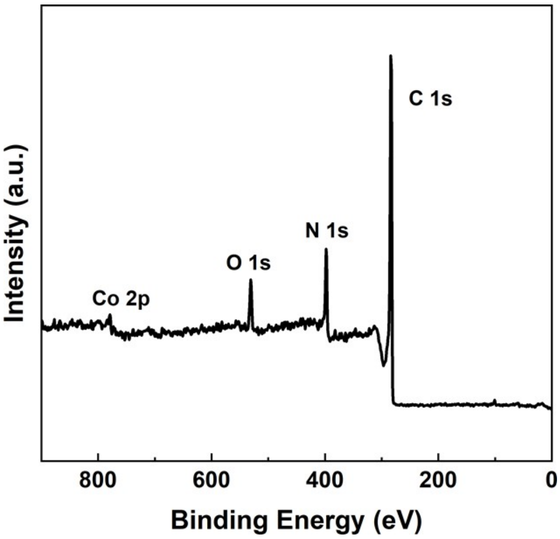

Fig. S4 The survey XPS spectrum of Co-N/CNTs-0.06

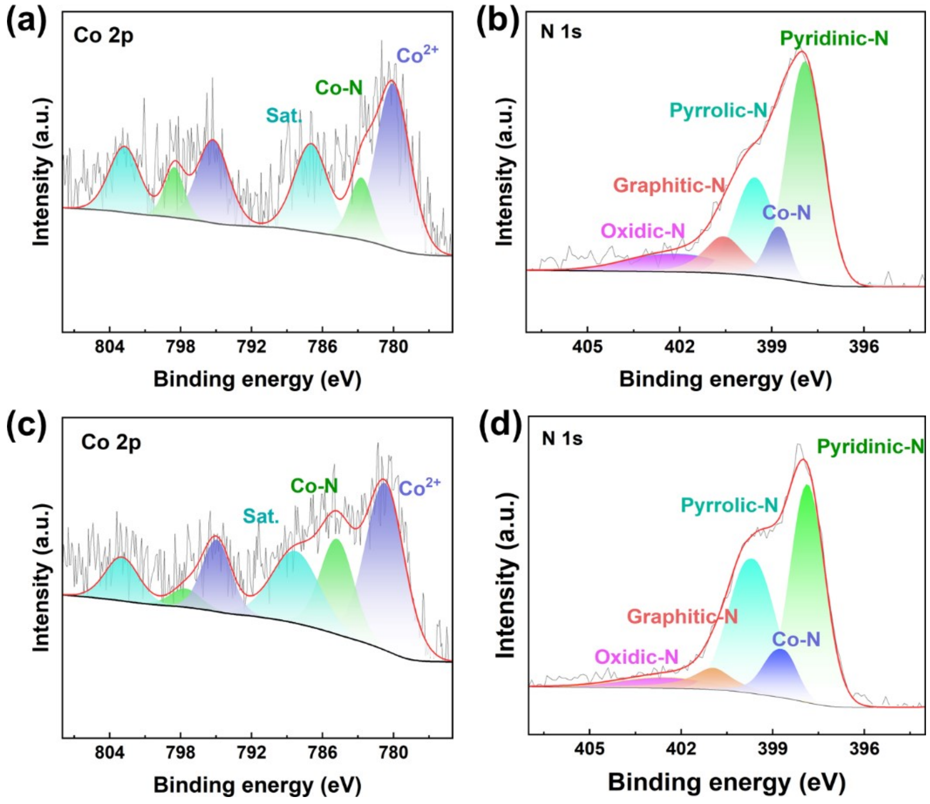

Fig. S5 (a) Co 2p and (b) N 1s XPS spectra of Co-N/CNTs-0.04. (c) Co 2p and (d) N 1s XPS spectra of Co-N/CNTs-0.08.

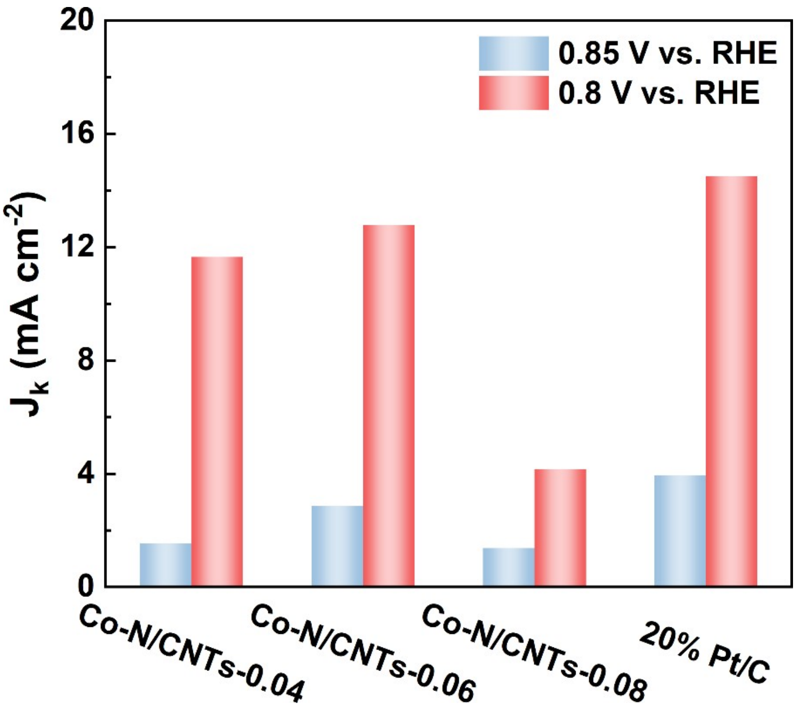

Fig. S6 J_k at 0.8 and 0.85 V of Co-N/CNTs-0.04, Co-N/CNTs-0.06, Co-N/CNTs-0.08 and 20% Pt/C.

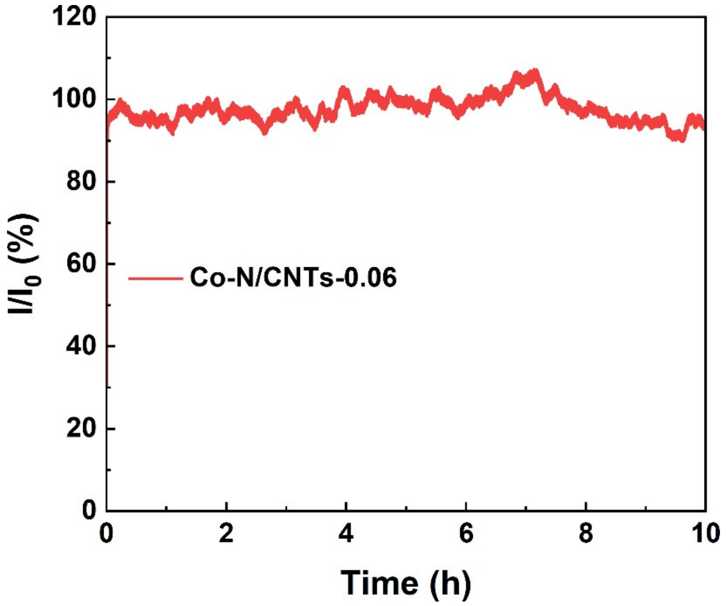

Fig. S7 Current retention from chronoamperometric curves of Co-N/CNTs-0.06 at 0.46 V vs. RHE in 0.1 M KOH for ORR.

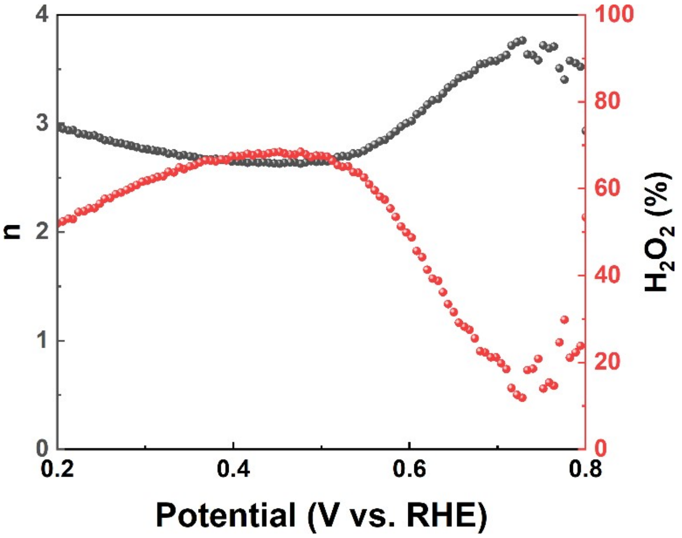

Fig. S8 Calculated n and determined H_2O_2% of CNTs at various potentials based on the RRDE.

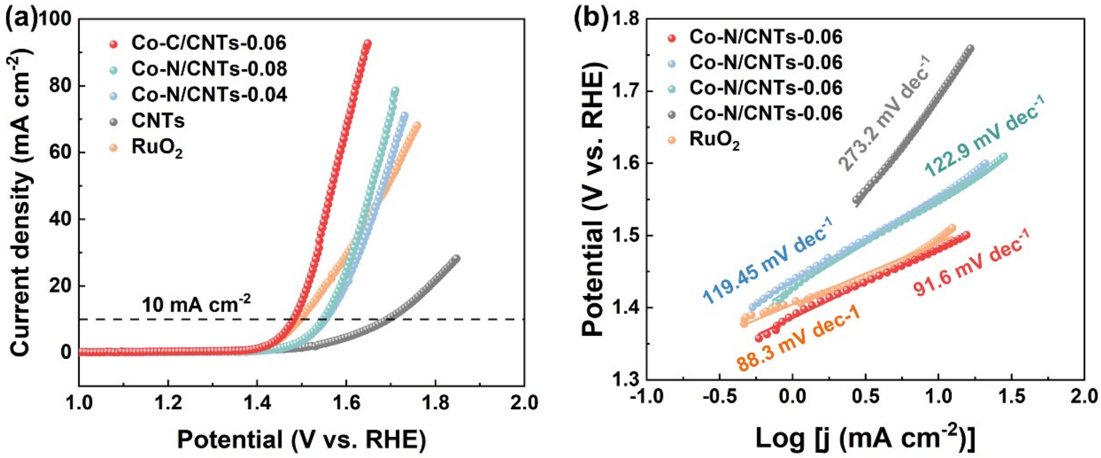

Fig. S9 (a) OER polarization curves of Co-N/CNTs-0.04, Co-N/CNTs-0.06, Co-N/CNTs-0.08 and RuO_2 in 1 M KOH, and (b) corresponding Tafel plots.

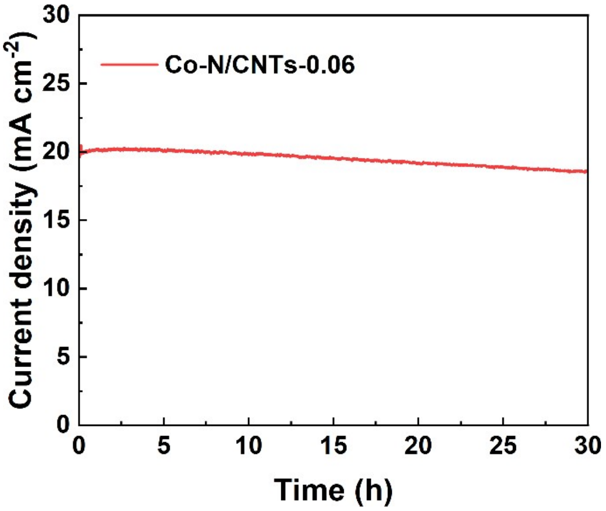

Fig. S10 Chronoamperometric curve of Co-N/CNTs-0.06 at Co-N/CNTs-0.06 at 1.51 V vs. RHE in 1.0 M KOH for OER.

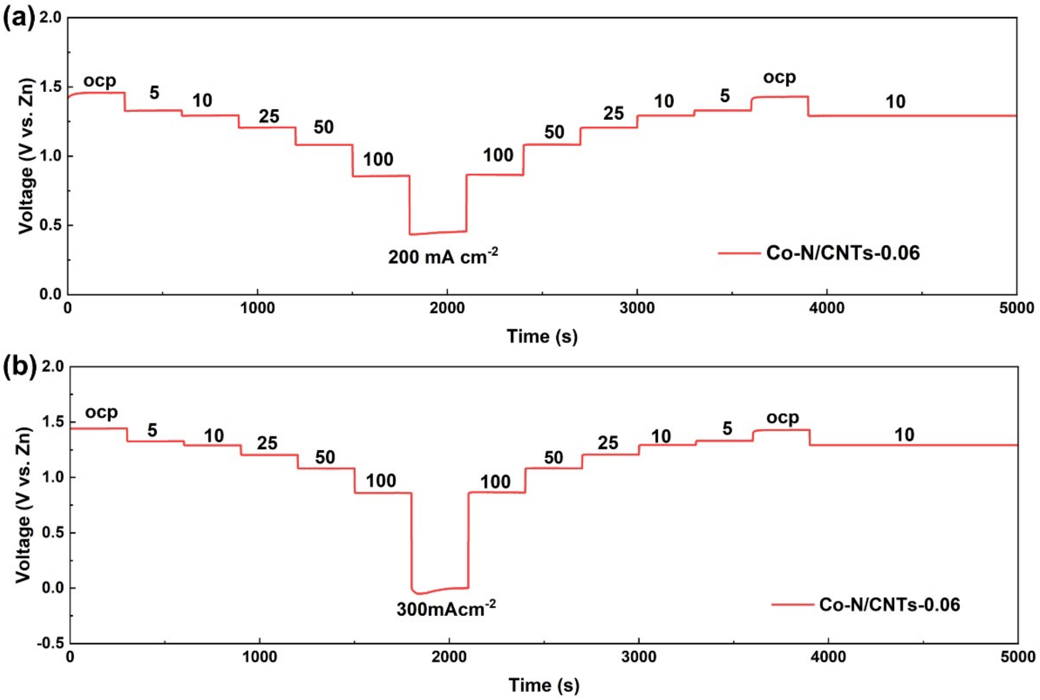

Fig. S11 Galvanostatic discharge curves at various current density, including (a) OCP-100 mA cm^{-2} and (b) OCP-300 mA cm^{-2}.

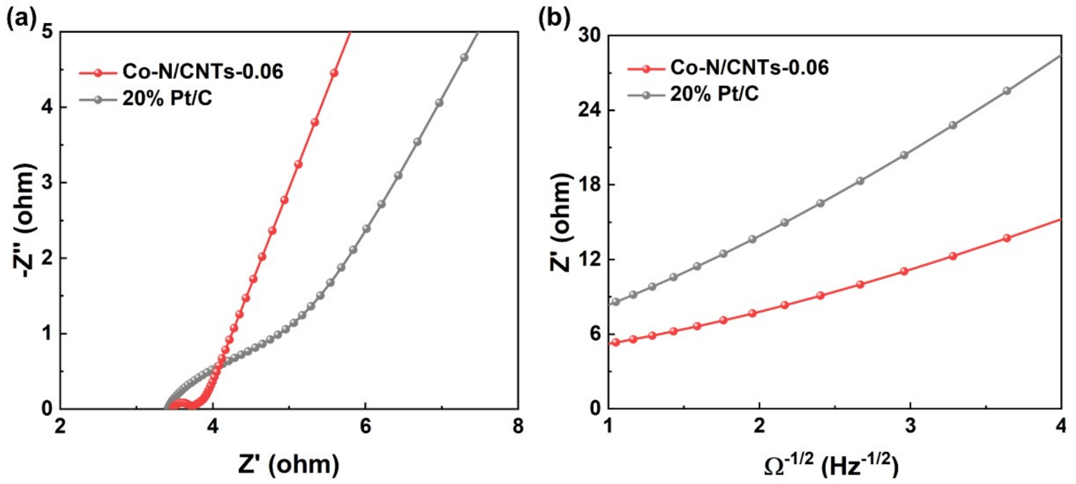

Fig. S12 (a) EIS of the Co-N/CNTs-0.06-based and 20% Pt/C-based ZAB. (b) Plots of Z′ vs. $\omega^{-1/2}$ calculated from EIS of Co-N/CNTs-0.06-based and 20% Pt/C-based ZAB.

Table. S1 Mass ratios of Co of Co-N/CNTs-0.06 obtained by ICP-MS testing

Catalysts	Co 2p (wt.%)
Co-N/CNT-0.06	0.86

Table. S2 Atomic ratios of Co and N species on the surface of Co-N/CNTs-0.04, Co-N/CNTs-0.06 and Co-N/CNTs-0.08 calculated by XPS spectra fitting

Catalysts	Co 2p (at.%)	N 1s (at.%)
Co-N/CNTs-0.04	0.43	3.22
Co-N/CNTs-0.06	0.61	6.41
Co-N/CNTs-0.08	1.12	9.10

Table. S3 Comparison of ORR catalytic activity

Catalysts	Half-wave potentials (V vs. RHE)	onset potentials (V vs. RHE)	References
Co-NCNT/Ng-900	0.83	-	1
$Co_{0.80}$NBC	0.86	1.02	2
Co_4N@d-NCNWs/D	0.83	0.93	3
CoSAs/N-CNS	0.91	0.98	4
Co–N@ACS	0.99	0.86	5
Co_4N/PNC-920	0.86	-	6
NC-Co SA	0.87	1.00	7
CoFe-Co@PNC-12	0.89	1.03	8
0.4Co@NC-900	0.91	-	9
Co-NC@NC	0.89	0.97	10
DAP-DAM-Co(NO3)2	0.90	1.02	11
Co/N-PCM	0.83	-	12
Co-N/CNTs-0.06	0.83	1.09	This work

References

1. K. Fu, Y. Wang, L. Mao, X. Yang, J. Jin, S. Yang and G. Li, *Chem. Eng. J.*, 2018, **351**, 94-102.
2. X. Wu, G. Han, H. Wen, Y. Liu, L. Han, X. Cui, J. Kou, B. Li and J. Jiang, *Energy Environ. Mater.*, 2022, **5**, 935-943.
3. C. Zhang, N. Huang, Z. Zhai, L. Liu, B. Chen, B. Yang, X. Jiang and N. Yang, *Adv. Energy Mater.*, 2023, **13**, 2301749.
4. D. Wang, M. Yuan, J. Xu, Y. Li, K. Shi, H. Yang, H. Li and G. Sun, *ACS Sustainable Chem. Eng.*, 2021, **9**, 16956-16964.
5. B. Zhou, Y. Liu, X. Wu, H. Liu, T. Liu, Y. Wang, S. Mehdi, J. Jiang and B. Li, *Nano Res.*, 2022, **15**, 1415-1423.
6. B. Li, Y. Ren, G. Zhang, C. Lv, L. Li, X. Yang, Z. Lu, X. Zhang and X. Yu, *Appl. Surf. Sci.*, 2025, **679**, 161212.
7. W. Zang, A. Sumboja, Y. Ma, H. Zhang, Y. Wu, S. Wu, H. Wu, Z. Liu, C. Guan, J. Wang and S. J. Pennycook, *ACS Catal.*, 2018, **8**, 8961-8969.
8. Z. Lei, Y. Tan, Z. Zhang, W. Wu, N. Cheng, R. Chen, S. Mu and X. Sun, *Nano Res.*, 2021, **14**, 868-878.
9. G. Zhou, X. Yan, T. Zhang, K. Wang, J. Zhang and J. Guo, Appl. Surf. Sci., 2023, 621, 156906.
10. W. Xi, W. Liu, A. Yu, M. Mu, W. Gu and L. Shi, Int. J. Hydrogen Energy, 2024, 72, 141-148.
11. T. Chen, C. Hao, Z. Chen, J. Li, C. Lin, P. K. Shen and Z. Q. Tian, Chem. Eng. J., 2025, 505, 159449.
12. F. Tang, Z. Wang, S. Wang, S. Xing, C. Li, S. Wang, Z. Jin and J.-B. Baek, Chem. Eng. J., 2024, 487, 150433.